ACS OMEGA

Open Access

http://pubs.acs.org/journal/acsodf

Article

Functionalization of Nanodiamond Surfaces with Metal β-Diketonato Complexes with Possible Application in Cancer Treatment

Siyanda Khoza, Anke Wilhelm, Elizabeth Erasmus,* and Eleanor Fourie*

Cite This: ACS Omega 2024, 9, 46217−46223

Read Online

ACCESS | Metrics & More | Article Recommendations | Supporting Information

ABSTRACT: Nanodiamonds (NDs) are used more frequently as drug carriers through absorption or chemical modification. In this report, we describe the chemical binding of metal β-diketonato complexes onto the ND surface using an aminosilane linker. The metals used were iron(III) and copper(II), with β-diketones, acetylacetone, trifluoroacetylacetone, and the naturally occurring curcumin, which is known for its biological activity. Improved cytotoxicity was observed with metal complexes bound to the drug carrier compared to the free metal complexes as a result of increased stability when bound to a carrier. The curcumin-containing copper(II) conjugate demonstrated an IC_{50} of 1.85 μM against the HeLa cell line and showed no toxicity in a larval zebrafish bioassay.

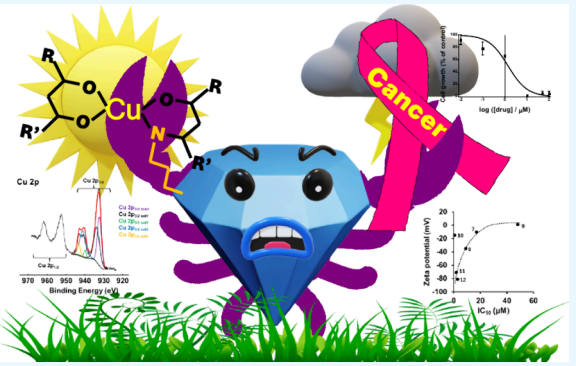

INTRODUCTION

Carbon-based materials offer a variety of versatile materials, of which nanomaterials have become an important field.[1] Among these, nanodiamonds (NDs) are significant due to their unique and stable structure of sp^2 hybridized carbon atoms. NDs are commercially produced through a detonation process and then purified using liquid oxidants such as acids, resulting in a surface rich in oxygen-containing functional groups such as carboxyl and hydroxyl groups. It also has a very small size distribution around 4−5 nm, giving more control over the substance, depending on its purpose.[2,3]

NDs are ideal for biological purposes due to their stable carbon structure. The biocompatibility of these materials has been widely investigated, especially the effect and safety on neural cells.[1,4] It is commonly employed as a drug delivery system,[5−7] usually by adsorbing or coating the relevant drug onto the material.[7,8] Alternatively, the desired drug can be chemically bonded to the surface of the ND.[9] The surface of the ND is rich in functional groups, making it easy to modify it for a variety of purposes. These include hydroxy-, amine-, nitro-, and other groups.[2,3,10] NDs are of particular interest as a chemotherapeutic drug delivery system due to their ability to improve drug stability and target cancer cells (both actively and passively, through the enhanced permeability and retention (EPR) effect).[5,11]

β-Diketones are of interest in anticancer studies due to their versatility as a synthetic scaffold, which can be modified to contain a large number of useful groups.[12] They are also easily complexed with many metals. The naturally occurring β-diketone, curcumin, is known to be biologically active but also offers valuable β-diketonato properties like metal binding.[13] These ligands can be easily complexed with cytotoxically active metals, thus increasing the cytotoxicity synergistically.[14−16] Metal β-diketonato complexes of metals such as iron(III) and copper(II) are easily synthesized but have also been shown to offer excellent cytotoxic possibilities.[14−16] In this study, β-diketonato complexes of iron(III) were first studied as a model due to their ease of use. This was followed by the study of copper(II) complexes, which aimed at superior cytotoxicity.

The previous study reported the anchoring of a cisplatin-like drug onto the ND through an aminosilane-linker.[9] It was found that the use of a silane-linker extended the amine group away from the surface of the ND and improved the availability and success of the drug/carrier conjugate. In this study, we utilize the aminosilane-linker to bond β-diketonato-containing iron(III) and copper(II) complexes to the ND. The β-diketones used are acetylacetone (acac), trifluoroacetylacetone (tfaa), and curcumin (cur). The objective of this study is to develop a drug/carrier conjugate system with high cytotoxicity while reducing the toxicity to the biological system by using the natural ligand, curcumin. The study reports on the synthesis and characterization of these new conjugates, as well as

Received: July 25, 2024
Revised: October 8, 2024
Accepted: October 11, 2024
Published: November 4, 2024

cytotoxicity results on HeLa cells and toxicity results on zebrafish larvae.

EXPERIMENTAL SECTION

Materials and Spectroscopic Characterization. Detonation NDs were purchased from Gansu Lingyun Corp., Lanzhou, China. Solid and liquid reagents were purchased from Merck and Sigma-Aldrich and were used without further purification unless stated otherwise.

Attenuated total reflection-Fourier transform infrared (ATR-FTIR) spectra were obtained from a Nicolet IS50 ATR Fourier transform spectrometer. UV/vis characterization of the modified NDs in suspension was measured on an Olis Clarity CCD UV/vis spectroscopic system using concentrations of 0.001 mg/mL acetonitrile and ethanol. X-ray photoelectron spectroscopy (XPS) measurements were conducted on a PHI 5000 Versaprobe system equipped with a monochromatic Al K_α X-ray source (Al K_α = 1486.6 eV). Operating conditions and settings are similar as reported in previous work from this lab.[17,18]

ICP-OES analysis was performed by IGS Laboratory Services, UFS. ND samples were digested by H_2SO_4 before analysis. Results were reported as milligrams per liter solution provided. This was converted to weight %.

Modification of Functional Groups on the ND Surface. The ND surface was modified in three steps via carboxylated and hydroxylated surfaces to form the silane-modified ND, ND−O−Si−C_3−NH_2, according to previously published procedures.[9]

Synthesis of Iron(III) and Copper(II) β-Diketonato Complexes (1−6). Metal complexes (**1**−**6**) were synthesized from the corresponding metal salt and β-diketone, according to published procedures.[19−21] Characterization data for **1**−**3** is summarized in Table 1, and data for **4**−**6** is summarized in Table 2.

Table 1. Characterization of Iron(III) β-Diketonato Complexes

compound	yield	reported UV max (nm)	reported IR peaks
[Fe(acac)$_3$] (**1**)	78%	270	1577, 1529
[Fe(tfaa)$_3$] (**2**)	67%	271	1737, 1611
[Fe(cur)$_3$] (**3**)	79%	422	3500−3396, 1596, 1508, 1385

Table 2. Characterization of Copper(II) β-Diketonato Complexes

compound	yield	reported UV max (nm)	reported IR peaks (cm^{-1})
[Cu(acac)$_2$] (**4**)	74%	295	1576, 1968, 2922
[Cu(tfaa)$_2$] (**5**)	74%	271	1473, 1608, 1736, 2939
[Cu(cur)$_2$] (**6**)	81%	422	1427, 1505, 1587

Anchoring of the Metal β-Diketonato Complexes onto the ND Surface. Metal β-diketonato complexes were anchored to the ND through a modified literature procedure.[22] Metal complexes (**1**−**6**, 1.5 mmol) were added to a suspension of amino-functionalized ND (0.1 g) in toluene (10 mL). The mixture was refluxed for approximately 16 h at 110 °C. The mixture was filtered and washed three times with isopropanol, and the precipitate was dried using vacuum.

Characterization of Tris(acetylacetonato)iron(III)-Modified ND, ND−O−Si−C_3−(NH(CH_3)CCHCOCH$_3$)−Fe-(acac)$_2$, 7. FTIR: 1020, 1107, 1560, 1608, 1656, and 3412 cm^{-1}. ICP-OES: 9.47 wt % Fe.

Characterization of Tris(trifluoroacetylacetonato)-iron(III)-Modified ND, ND−O−Si−C_3−(NH(CH_3)-CCHCOCF_3)−Fe(tfaa)$_2$, 8. FTIR: 1033, 1131, 1527, 1609, and 3348 cm^{-1}. ICP-OES: 12.96 wt % Fe.

Characterization of Tris(curcumin)iron(III)-Modified ND, ND−O−Si−C_3−NH−Fe(cur)$_3$, 9. FTIR: 1150, 1267, 1491, 1587, and 3492 cm^{-1}. ICP-OES: 1.46 wt % Fe.

Characterization of Tris(acetylacetonato)copper(II)-Modified ND, ND−O−Si−C_3−(NH(CH_3)CCHCOCH$_3$)−Cu-(acac), 10. FTIR: 1255, 1373, 1429, 1561, and 3339 cm^{-1}. ICP-OES: 9.12 wt % Cu.

Characterization of Tris(trifluoroacetylacetonato)-copper(II)-Modified ND, ND−O−Si−C_3−(NH(CH_3)-CCHCOCF_3)−Cu(tfaa), 11. FTIR: 1028, 1195, 1092, 1257, 1297, 1451, 1531, 1619, and 3354 cm^{-1}. ICP-OES: 14.80 wt % Cu.

Characterization of Tris(curcumin)copper(II)-Modified ND, ND−O−Si−C_3−NH-Cu(cur)$_2$, 12. FTIR: 1028, 1155, 1259, 1505, 1598, 1973, and 3383 cm^{-1}. ICP-OES: 0.46 wt % Cu.

Biological Testing. *Cell Culture.* Ethical clearance for this work was obtained from the UFS Environmental & Biosafety Research Ethics Committee under project UFS-ESD2023/0015/23. The human cervical cancer cell line (Hela cell line) was grown with 10% fetal calf serum and 1% penicillin/streptomycin in Dulbecco's modified Eagle's medium (DMEM). The cells were incubated at 37 °C in a humidified environment of 5% carbon dioxide.

Cytotoxicity Test. A monolayer of cells was trypsinized, centrifuged, and resuspended in 1 mL of growth medium.[23] The suspension was diluted to 0.5 × 10^5 cells per mL. From this suspension, 0.1 mL was added to each well of a 96-well microplate. Plates were incubated for 1 h to adhere cells to the plate. Dilutions of functionalized NDs were prepared (concentrations used per active metal content, as determined by ICP-OES) and added (0.1 mL) to each well. The plates were incubated at 37 °C with 5% carbon dioxide for 3 days. The incubation period was concluded by the addition of trichloroacetic acid (0.05 mL of 50%), and the plates were stored overnight in the fridge. Plates were washed under flowing tap water and dried at 50 °C for 1 h. SRB stain (0.1 mL) was added to each well and stored in the dark for 30 min. The plates were washed with 1% acetic acid (0.1 mL × 4), dried, and 0.1 mL (10 mM) tris buffer (tris(hydroxymethyl)-aminomethane) was added to each well. Plates were gently shaken for 1 h, and absorbance was measured at 510 nm. The growth inhibition was determined as a percentage of the control group's optical density. GraphPad Prism version 5.00 software, San Diego, California, USA, was used to determine IC_{50} values by nonlinear regression versus a normalized response.

Toxicity Testing Using Zebrafish Larvae. Ethical clearance for this work was obtained from the UFS Animal Research Ethics Committee under the project UFS-AED2022/0013/22. Zebrafish were kept under standard conditions at the Department of Genetics and were bred by Alistair Naidoo and hatched by Dr. Anke Wilhelm. Eggs were collected from the Department of Genetics and cautiously transported to the Department of Chemistry, where the eggs were cleaned,

https://doi.org/10.1021/acsomega.4c06835
ACS Omega 2024, 9, 46217−46223

Scheme 1. Synthetic Route for the Preparation of ND/Metal β-Diketonato Conjugates (7−12)

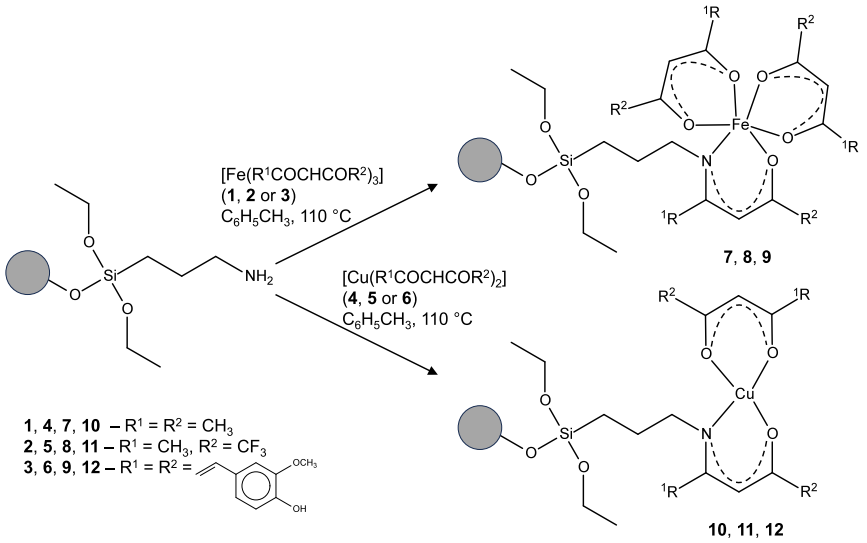

separated into Petri dishes, and incubated at 28.5 °C in an E3 medium (0.5 mM NaCl, 0.17 mM KCl, 0.33 mM $CaCl_2$, and 0.33 mM $MgSO_4$) in water (0.5 mL methylene blue 0.05% w/v was added to 1 L medium as a disinfectant; pH was corrected to 7.4 by K_2CO_3 0.5 M) which was changed every 24 h over a 7-day period. Unfertilized eggs and dead larvae were removed daily (if present). The modified ND samples were suspended in DMSO (10 mg/mL) as a stock solution for the toxicity tests.

Toxicity Test. Larvae were incubated with the sample suspension and individually checked under a microscope at four-time intervals to correctly identify the maximum tolerated concentration (MTC).

The tests were performed 7 days post fertilization (dpf) for each extract sample at 100, 50, 25, 12.5, 6.25, and 3.125 μM (from the stock solution with the E3 medium as the dilutant). Zebrafish larvae were incubated in a 96-well setup with ND samples (50 and 200 μL E3 medium) and were individually observed under a microscope (×30 magnification) over a period of four-time intervals (1.5, 3, 6, and 24 h). The larvae that presented with locomotor impairments (body deformation, loss of larval motion, or death) were recorded and compared to the control group (untreated larvae). The MTC was characterized by no more than two out of 12 compromised larvae and was then taken as the highest test concentration in the activity test.

RESULTS AND DISCUSSION

Preparation. The surface of NDs was modified by attaching an aminated silane functional group (ND−O−Si−C_3−NH_2).[9] The iron(III) β-diketonato complexes, [Fe(acac)$_3$] (**1**), [Fe(tfaa)$_3$] (**2**), and [Fe(cur)$_3$] (**3**), as well as the copper(II) complexes, [Cu(acac)$_2$] (**4**), [Cu(tfaa)$_2$] (**5**), and [Cu(cur)$_2$] (**6**), were prepared according to literature methods.[14,21,22,24] All the metal complexes synthesized are paramagnetic in nature; thus, no NMR could be measured. Structural confirmation was carried out by comparing FTIR and UV/vis data with the literature data. The metal complexes were anchored to the ND surface through a reaction with the amine group under reflux in toluene overnight, as shown in Scheme 1. This reaction leads to the formation of an amine bond, where one β-diketonato oxygen atom is replaced with the ND-linked nitrogen. This method is commonly employed in anchoring β-diketonato complexes onto silicon wafers.[22] Conjugates prepared in this study (**7**−**12**) were characterized by FTIR, UV/vis, and XPS spectroscopy. Additionally, SEM (scanning electron microscopy) analysis, zeta potential, and particle size analysis were performed.

The ATR-FTIR spectra of iron(III) (**7**−**9**) and copper(II) (**10**−**12**) containing conjugates, shown in parts S1 and S2, indicate the anchoring of the metal complexes to the NDs. The FTIR spectra of the conjugates show significant signals coming from the ND (broad O−H stretching ∼3300 to 3100 cm^{-1}) and the APTMES linker (∼1100 to 1000 cm^{-1}), as well as stretching frequencies attributed to the metal complexes. The metal complexes are identifiable by vibrations attributed to the β-diketonato ligands such as C═O and C−H (1500−1700 cm^{-1}). C−F stretches are also evident at 1300−1000 cm^{-1} for the fluorine-containing complexes **8** and **11**. These signals show a slight shift of the peaks from the free metal complex as a result of binding.

UV/vis spectra of conjugates **7**−**12** were measured in a 1:1 mixture of ethanol and acetonitrile and are shown in Figure S3. These spectra indicate anchoring of the metal complexes to the NDs, as the UV/vis components of both the NDs and the metal complexes are present, albeit slightly shifted. The spectra show a broad nanoND-based absorption from 200 to 600 nm. Absorption maxima are also observed between 250 and 450 nm, attributed to the absorption component of the bound metal β-diketonato complexes, at similar wavelengths to that of the free complexes.

XPS. XPS is a technique utilized to determine the surface environment of the elements present and the oxidation states of metals. Figure 1A shows the C 1s region of the silane-modified ND (ND−O−Si−C_3−NH_2) as a representative example of the C 1s XPS. The majority of the carbon C 1s photoelectron lines measured for all the modified ND conjugates are present in the sp^2 and sp^3 hybridized states associated with the bulk carbon diamond structure (as well as a small amount of adventitious carbon). The remaining part of the photoelectron envelope was fitted with simulated peaks for Si−C, C−O, and C−N belonging to the silane. When the β-diketonato metal complexes are anchored to the NDs, only the C−F photoelectron line (of **8** and **11**, see Figure 1A for **8**),

https://doi.org/10.1021/acsomega.4c06835
ACS Omega 2024, 9, 46217−46223

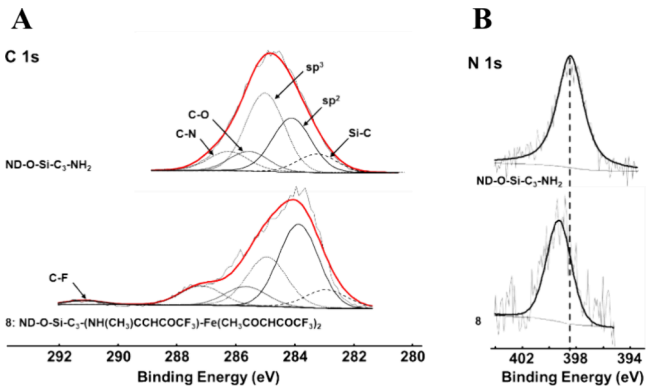

Figure 1. XPS of the (A) C 1s and (B) N 1s region indicating the different chemical environments of the silane-modified ND, ND−O−Si−C_3−NH_2, and the Fe-ND-conjugate **8**.

which has a highly electronegative environment, can be distinguished. The other photoelectron lines of the β-diketo ligand (C−O, C−C, and C−H) are merged with the simulated peaks of ND−O−Si−C_3−NH_2. Upon anchoring of the metal complex to the ND via the amine group of the silane, the C−N photoelectron line shifted to more positive binding energies due to the influence of the metal bound to the N (M−N−C), confirming the proposed binding mode. This positive shift was also observed in the N 1s when comparing the binding energy of ND−O−Si−C_3−NH_2 (398.4 eV) with the metal-anchored NDs (**7**−**11**, at ∼399.2 eV), see Figure 1B for **8** as an example.

The main Fe $2p_{3/2}$ photoelectron lines of the iron metal center were found at 710.6, 710.9, and 710.7 eV for **7**−**10**, respectively (see Figure 2A for **8** as an example). The

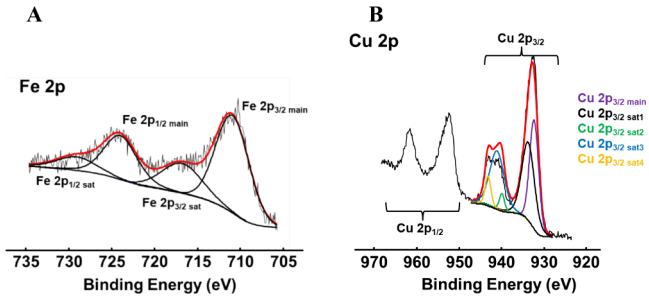

Figure 2. XPS spectra of the (A) Fe 2p (of **8**) and (B) Cu 2p (of **11**) regions, indicating the simulate fits.

corresponding main Fe $2p_{1/2}$ photoelectron lines were located at ca. 13.1 eV higher binding energies than the Fe $2p_{3/2}$ photoelectron lines. The Fe 2p photoelectron envelope also included shakeup peaks, which are present at ca. 5 eV higher than the main photoelectron lines. The presence of the shakeup lines indicates that the iron is present as Fe(III), this is further confirmed by the position of the Fe $2p_{3/2}$ photoelectron lines at ca. 710.7 eV. This correlates with the binding energies reported for Fe(III) in literature.[22,25]

The XPS analysis of the ND conjugates **10**−**12** reveals a Cu 2p photoelectron envelope with multiple features. The Cu $2p_{3/2}$ main photoelectron line is present as a sharp and well-defined line, located at ca. 932.3, 932.5, and 932.4 eV for **10**−**12**, respectively (see Figure 2 B for **11** as an example). The peak separation between the Cu $2p_{3/2}$ and Cu $2p_{1/2}$ photoelectron lines is approximately 20 eV. Complex satellite features are found a few eV higher than the main photoelectron lines. The satellite feature consists of multiple overlapping lines with varying intensities. Following Biesinger's proposal,[26] four simulated peaks were fitted using a specific ratio for the satellite structure. As reported in previous studies, the peak position is influenced by the electronic and structural environment of the Cu(II).[27−29]

SEM. SEM and energy dispersive spectroscopy (EDS) analyses were performed on all conjugates **7**−**12**. SEM images of curcumin-containing conjugates **9** and **12** are shown in Figure 3 (SEM images of conjugates **7**−**8** and **10**−**11** are presented in Figures S4 and S5). The images show that the nanoparticles retain the irregular, nongeometric shape and nanostructure, with a particle size of less than 50 nm. No visible modification of the surface is expected since chemical binding of the metal complexes occurs at the molecular level and is therefore not observable by SEM. Some aggregation is visible in the SEM images shown. This is however a solid-state effect since SEM is performed on solid samples. The ND conjugates disperse successfully when in suspension, as validated by zeta potential results. EDS analysis confirmed the presence of C, O, N, Si, and either Fe or Cu for **7**−**12**.

Zeta Potential, ζ. As the NDs **7**−**12** will be tested for their potential anticancer activity, it is crucial that they remain in a colloidal suspension and do not settle. To assess the impact of anchored metal β-diketonato conjugates on the stability and potential interactions of the modified NDs in a dispersion, the zeta potentials (ζ) were measured at biological pH and saline concentration (Table 3).

Materials with $|\zeta|$ less than 30 mV typically result in unstable suspensions, where particles are prone to coagulation and settle out of solution. Conversely, colloidal suspensions with $|\zeta|$ greater than 30 mV tend to be stable, as the strong electrostatic repulsion between the particles prevents aggregation.[30] In this context, the curcumin iron ND (**9**) exhibits a ζ value near neutrality, indicating high instability in suspension and a strong likelihood of settling out of the suspension. Similarly, the NDs containing the acetylacetonate conjugates of Fe (**7**) and Cu (**10**) have $|\zeta|$ values below 30 mV, indicating that these suspensions are not stable. However, the Cu-conjugates (**11**−**12**) generally possess more negative zeta-potentials than their Fe counterparts, signifying stronger electrostatic stability. Among them, **11** and **12** demonstrate the most stable suspensions.

Biological Screening. The ND conjugates (**7**−**12**) prepared in this study are aimed for use in the treatment of cancer as a drug delivery system for the β-diketonato metal drug. The cytotoxicity of all drug/carrier conjugates (**7**−**12**) was determined against the HeLa cell line by utilizing the SRB (sulforhodamine B) assay.[23] Concentrations of drugs loaded on the carrier were determined from ICP-OES analysis based on the amount of metal center present. For comparative purposes, all free metal β-diketonato complexes (**1**−**6**) were also tested under our conditions. Cisplatin was tested under our conditions as a positive control, and the IC_{50} was determined as 2.83 μM. The IC_{50} values (concentration needed for 50% cancer cell death) of **1**−**12** are summarized in Table 4, and survival curves of the curcumin-containing conjugates **9** and **12** against HeLa cells are shown in Figure 4.

Previous work has demonstrated that the ND drug carrier exhibits no significant cytotoxicity, making it ideal for use as a drug carrier.[9] In general, the copper(II) complexes (**4**−**6**) possess significantly better cytotoxicity (lower IC_{50}) than their iron(III) counterparts (**1**−**3**). In general, the anchoring of the

https://doi.org/10.1021/acsomega.4c06835
ACS Omega 2024, 9, 46217−46223

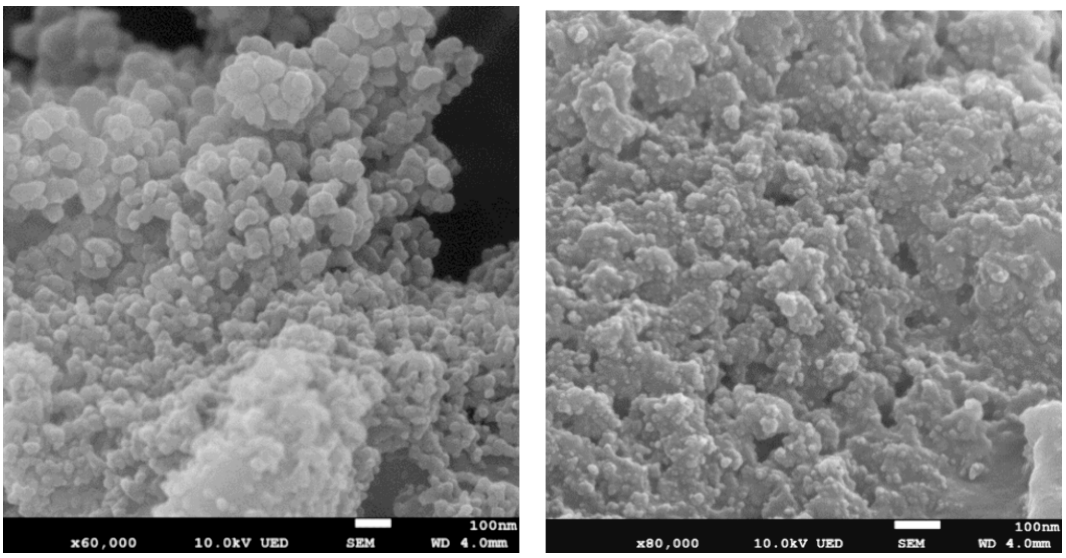

Figure 3. SEM images of curcumin-containing drug-carrier conjugates **9** and **12**.

Table 3. Zeta-Potentials of 7−12 Measured at Biological pH and Saline Concentration

	XPS atomic %		
conjugate	C	metal	zeta potential, ζ (mV)
7	96.31	3.69	−10
8	99.63	0.37	−35
9	97.84	2.16	1
10	98.47	1.53	−15
11	98.41	1.59	−81
12	99.18	0.82	−71

metal drug onto the ND carrier increased the cytotoxicity of the conjugate. This can be attributed to its ability to stabilize the drug and protect it from decomposition. By anchoring it onto the drug carrier, it is more successfully delivered to the cancer cell. Thus, by reducing the time taken to delivery, the time for possible degradation is also reduced. Additionally, by anchoring the complex onto the carrier, the carrier can sterically protect the compound from being broken down in the biological system. It also illustrates the ability of the carrier to deliver the drug more directly to the cancerous cell. Incorporating the naturally occurring curcumin, with its variety of health benefits,[31] did not significantly increase the cytotoxicity of the metal complexes (**3**, **6**) or the drug/carrier conjugate (**9**, **12**). Although the copper(II) curcumin conjugate (**12**) did exhibit excellent cytotoxicity, comparable to that of cisplatin.

The results indicate that as the zeta potential of the ND conjugates became more negative ($|\zeta|$ increases), the IC_{50} value of the ND conjugates decreases (see Figure 5). This suggests that the more stable the ND suspension is, the more cytotoxic the ND conjugate becomes. Therefore, if the ND conjugate remains in suspension and does not settle, cellular uptake of the ND conjugate is positively affected. In addition, cancer cells have an extracellular pH of 6.7−7.1, creating a positive environment, that may attract the negatively charged ND conjugates more effectively, resulting in improved cytotoxicity.

Toxicity studies were conducted on zebrafish larvae since it is a useful model for vertebrate systems and shows significant similarity to the human genome. The MTCs (the highest concentration of a substance that a biological system can withstand without showing adverse effects) of drug/carrier conjugates **7**−**12** were determined. The MTC values were obtained by subjecting zebrafish larvae to various concentrations of the synthesized conjugates and observing the concentrations at which no negative effects were experienced. MTC values are summarized in Table 4.

All drug/carrier conjugates showed low toxicity, except for the copper(II) acetylacetonato derivative (**10**) which was highly toxic. Conjugates containing the naturally occurring curcumin were found to show no negative effects on zebrafish larvae, even at the highest concentration tested. The curcumin-containing copper conjugate (**12**) showed excellent cytotoxicity (IC_{50} = 1.85 μM), while it had no toxicity. Figure 6 shows a zebrafish larva in a completely unaffected and healthy state in

Table 4. IC_{50} and MTC Values Determined against HeLa Cells of Free Metal β-Diketo Complexes and Metal β-Diketo-Containing ND Conjugates

$[M(\beta\text{-dik})_{2/3}]$	IC_{50} (μM)	ND-NH-$[M(\beta\text{-dik})_{2/3}]$	IC_{50} (μM)	MTC (μg/mL)	ζ (mV)
1	23.8 ± 1.5	**7**	14.71 ± 1.5	50	−10
2	25.1 ± 1.5	**8**	15.91 ± 1.4	50	−35
3	84.7 ± 1.4	**9**	53.0 ± 1.6	100	1
4	3.31 ± 1.2	**10**	1.11 ± 1.3	1.5	−15
5	1.61 ± 1.1	**11**	7.73 ± 1.3	100	−81
6	3.73 ± 1.2	**12**	0.17 ± 1.4	100	−71
cisplatin	2.83 ± 1.5				

https://doi.org/10.1021/acsomega.4c06835
ACS Omega 2024, 9, 46217−46223

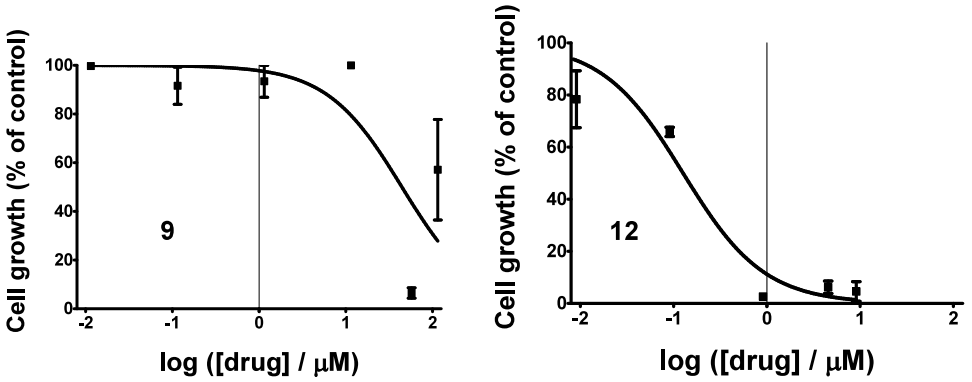

Figure 4. Cell growth curves of **9** (left) and **12** (right), showing the percentage of HeLa cell survival versus drug concentration.

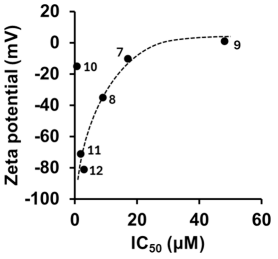

Figure 5. Graph showing the relationship between the zeta potential and IC_{50} values of **7**−**12**.

a suspension of the highest concentration of **12**, indicating its success.

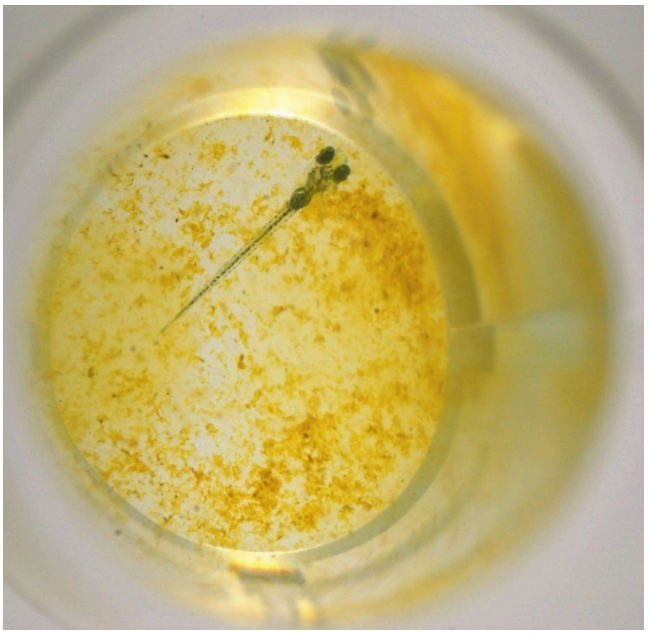

Figure 6. Zebrafish larvae in a suspension of **12**, showing high tolerance to the nanoparticle conjugate.

CONCLUSIONS

We report the synthesis of iron(III) and copper(II) β-diketo complexes supported on NDs as drug carriers. These metal complexes are chemically bonded to the ND surface via an aminosilane linker. Three different β-diketonato ligands are used, including acetylacetone, trifluoroacetylacetone, and naturally occurring curcumin. The presence of the metal complexes on the ND surface was confirmed by FTIR and UV/vis spectroscopy as well as SEM/EDS analysis. XPS analysis confirmed the metal oxidation states and was used to calculate the concentration of metal complexes present on the surface of the ND. Cytotoxicity of all conjugates was measured against HeLa cells, and toxicity was determined by a zebrafish essay. Excellent cytotoxicity was achieved, especially for copper(II)-containing conjugates. The curcumin-containing copper(II) conjugate showed excellent cytotoxicity with an IC_{50} of 1.85 μM and no toxicity (IC_{50} of cisplatin 2.83 μM). These preliminary screening results illustrate the potential of the synthesized conjugates as anticancer drugs. It is, however, only preliminary results and further investigation into stability, pharmacokinetics (how it is absorbed, distributed, metabolized, and excreted in a biological system), and potential side effects are crucial to confirm their efficacy and safety.

ASSOCIATED CONTENT

Supporting Information

The Supporting Information is available free of charge at https://pubs.acs.org/doi/10.1021/acsomega.4c06835.

Spectroscopic (FTIR and UV/vis) and SEM data of conjugates not shown in the publication and all cell growth curves of cytotoxic studies (PDF)

AUTHOR INFORMATION

Corresponding Authors

Elizabeth Erasmus − *Department of Chemistry, University of the Free State, Bloemfontein 9300, South Africa;* orcid.org/0000-0003-0546-697X; Phone: 27 51 4012071; Email: Erasmus@ufs.ac.za; Fax: 27 51 4017295

Eleanor Fourie − *Department of Chemistry, University of the Free State, Bloemfontein 9300, South Africa;* orcid.org/0000-0002-6696-6495; Phone: 27 51 4012071; Email: Fouriee@ufs.ac.za; Fax: 27 51 4017295

Authors

Siyanda Khoza − *Department of Chemistry, University of the Free State, Bloemfontein 9300, South Africa*

Anke Wilhelm − *Department of Chemistry, University of the Free State, Bloemfontein 9300, South Africa;* orcid.org/0000-0003-4561-5589

Complete contact information is available at: https://pubs.acs.org/10.1021/acsomega.4c06835

https://doi.org/10.1021/acsomega.4c06835
ACS Omega 2024, 9, 46217−46223

Funding

The author would like to acknowledge generous financial support from the National Nanoscience Postgraduate Teaching and Training Platform, Sasol and UFS during this study.

Notes

The authors declare no competing financial interest.

■ ACKNOWLEDGMENTS

The author would like to acknowledge generous financial support from the National Nanoscience Postgraduate Teaching and Training Platform, Sasol and UFS during this study.

■ REFERENCES

(1) Rauti, R.; Musto, M.; Bosi, S.; Prato, M.; Ballerini, L. Properties and behavior of carbon nanomaterials when interfacing neuronal cells: How far have we come? *Carbon* **2019**, *143*, 430−446.
(2) Mochalin, V. N.; Shenderova, O.; Ho, D.; Gogotsi, Y. The properties and applications of nanodiamonds. *Nat. Nanotechnol* **2012**, *7* (1), 11−23.
(3) Krueger, A. The structure and reactivity of nanoscale diamond. *J. Mater. Chem.* **2008**, *18* (13), 1485−1492.
(4) Vaitkuviene, A.; Ratautaite, V.; Ramanaviciene, A.; Sanen, K.; Paesen, R.; Ameloot, M.; Petrakova, V.; McDonald, M.; Vahidpour, F.; Kaseta, V.; et al. Impact of diamond nanoparticles on neural cells. *Mol. Cell Probe* **2015**, *29* (1), 25−30.
(5) Mu, W.; Chu, Q.; Liu, Y.; Zhang, N. A Review on Nano-Based Drug Delivery System for Cancer Chemoimmunotherapy. *Nano-Micro Letters* **2020**, *12* (1), 142.
(6) Xu, J.; Chow, E. K.-H. Biomedical applications of nanodiamonds: From drug-delivery to diagnostics. *SLAS Technology* **2023**, *28* (4), 214−222.
(7) Mochalin, V. N.; Pentecost, A.; Li, X.-M.; Neitzel, I.; Nelson, M.; Wei, C.; He, T.; Guo, F.; Gogotsi, Y. Adsorption of Drugs on Nanodiamond: Toward Development of a Drug Delivery Platform. *Mol. Pharmaceutics* **2013**, *10* (10), 3728−3735.
(8) Neburkova, J.; Vavra, J.; Cigler, P. Coating nanodiamonds with biocompatible shells for applications in biology and medicine. *Curr. Opin. Solid State Mater. Sci.* **2017**, *21* (1), 43−53.
(9) Fiekkies, J. T. R.; Fourie, E.; Erasmus, E. Cisplatin-functionalized nanodiamonds: preparation and characterization, with potential antineoplastic application. *Applied Nanoscience* **2021**, *11* (8), 2235−2245.
(10) Xing, Y.; Dai, L. Nanodiamonds for Nanomedicine. *Nanomedicine* **2009**, *4* (2), 207−218.
(11) Pan, F.; Khan, M.; Ragab, A. H.; Javed, E.; Alsalmah, H. A.; Khan, I.; Lei, T.; Hussain, A.; Mohamed, A.; Zada, A.; et al. Recent advances in the structure and biomedical applications of nanodiamonds and their future perspectives. *Materials & Design* **2023**, *233*, No. 112179.
(12) Jakob Kljun, I. T. B-Diketones as Scaffolds for Anticancer Drug Design−From Organic Building Blocks to Natural Products and Metallodrug Components. *Eur. J. Inorg. Chem.* **2017**, *2017* (12), 1655−1666.
(13) Tomeh, M. A.; Hadianamrei, R.; Zhao, X. A Review of Curcumin and Its Derivatives as Anticancer Agents. *Int. J. Mol. Sci.* **2019**, *20*, No. 1033.
(14) Khalil, M. I.; Al-Zahem, A. M.; Al-Qunaibit, M. H. Synthesis, Characterization, Mössbauer Parameters, and Antitumor Activity of Fe(III) Curcumin Complex. *Bioinorg. Chem. Appl.* **2013**, *2013*, No. 982423.
(15) Özbolat, G.; Yegani, A. A.; Tuli, A. Synthesis, characterization and electrochemistry studies of iron(III) complex with curcumin ligand. *Clin. Exp. Pharmacol. Physiol.* **2018**, *45* (11), 1221−1226.
(16) Mohammed, F.; Rashid-Doubell, F.; Taha, S.; Cassidy, S.; Fredericks, S. Effects of curcumin complexes on MDA-MB-231 breast cancer cell proliferation. *Int. J. Oncol.* **2020**, *57* (2), 445−455.
(17) Botha, E.; Landman, M.; van Rooyen, P. H.; Erasmus, E. Electronic properties of ferrocenyl-terpyridine coordination complexes: An electrochemical and X-ray photoelectron spectroscopic approach. *Inorg. Chim. Acta* **2018**, *482*, 514−521.
(18) Erasmus, E. X-ray photoelectron spectroscopy: Charge transfer in Fe 2p peaks and inner-sphere reorganization of ferrocenyl-containing chalcones. *J. Electron Spectrosc. Relat. Phenom.* **2018**, *223*, 84−88.
(19) Conradie, M. M.; van Rooyen, P. H.; Conradie, J. Crystal and electronic structures of tris[4,4,4-Trifluoro-1-(2-X)-1,3-butanedionato]iron(III) isomers (X = thienyl or furyl): An X-ray and computational study. *J. Mol. Struct.* **2013**, *1053*, 134−140.
(20) Joubert, C. C.; van As, L.; Jakob, A.; Speck, J. M.; Lang, H.; Swarts, J. C. Intramolecular electronic communication in ferrocene-based β-diketonato copper(II) complexes as observed by an electrochemical study. *Polyhedron* **2013**, *55*, 80−86.
(21) Refat, M. S. Synthesis and characterization of ligational behavior of curcumin drug towards some transition metal ions: Chelation effect on their thermal stability and biological activity. *Spectrochimica Acta Part A: Molecular and Biomolecular Spectroscopy* **2013**, *105*, 326−337.
(22) Conradie, M. M.; Conradie, J.; Erasmus, E. Immobilisation of iron tris(β-diketonates) on a two-dimensional flat amine functionalised silicon wafer: A catalytic study of the formation of urethane, from ethanol and a diisocyanate derivative. *Polyhedron* **2014**, *79*, 52−59.
(23) Vichai, V.; Kirtikara, K. Sulforhodamine B colorimetric assay for cytotoxicity screening. *Nat. Protoc.* **2006**, *1* (3), 1112−1116.
(24) Chiyindiko, E.; Conradie, J. Redox behaviour of bis(β-diketonato)copper(II) complexes. *J. Electroanal. Chem.* **2019**, *837*, 76−85.
(25) Conradie, J.; Erasmus, E. XPS Fe 2p peaks from iron tris(β-diketonates): Electronic effect of the β-diketonato ligand. *Polyhedron* **2016**, *119*, 142−150.
(26) Biesinger, M. C. Advanced analysis of copper X-ray photoelectron spectra. *Surf. Interface Anal.* **2017**, *49* (13), 1325−1334.
(27) Conradie, J.; Erasmus, E. XPS photoelectron lines, satellite structures and Wagner plot of Cu(II) β-diketonato complexes explained in terms of its electronic environment. *J. Electron Spectrosc. Relat. Phenom.* **2022**, *259*, No. 147241.
(28) Erasmus, E. Morphology-Dependent Ullmann C-O Arylation Using Cu2O Nanocrystals. *J. Nanomater.* **2020**, *2020* (1), No. 6726170.
(29) Zhou, Q.; Zhang, Y.; Zeng, T.; Wan, Q.; Yang, N. Morphology-dependent sensing performance of CuO nanomaterials. *Anal. Chim. Acta* **2021**, *1171*, No. 338663.
(30) Clogston, J. D.; Patri, A. K. Zeta potential measurement. *Methods Mol. Biol.* **2011**, *697*, 63−70.
(31) Surbhi Rathore, M. M.; Sharma, P.; Devi, S.; Nagar, J. C.; Khalid, M. Curcumin: A Review for Health Benefits. *Int. J. Res. Rev.* **2020**, *7* (1), 273−290.

https://doi.org/10.1021/acsomega.4c06835
ACS Omega 2024, 9, 46217−46223